Joint International Topical Meeting on Mathematics & Computation and Supercomputing in Nuclear Applications (M&C + SNA 2007)
Monterey, California, April 15-19, 2007, on CD-ROM, American Nuclear Society, LaGrange Park, IL (2007)

USE OF THE APOLLO2 CODE FOR BWR ASSEMBLY ANALYSIS

Laure Mondelain, Igor Zmijarevic, Jean Michel Do and Véronique Bellanger
Commissariat à l'Energie Atomique
DEN/DANS/DM2S
Service d'Etudes de Réacteurs et de Mathématiques Appliquées
Centre de Saclay
91191 Gif-sur-Yvette cedex, France
laure.mondelain@cea.fr, igor.zmijarevic@cea.fr, jean-michel.do@cea.fr, veronique.bellanger@cea.fr

ABSTRACT

The modular multigroup transport code APOLLO2 has been applied to BWR assemblies. The influence of the calculation options on the reactivity, pin power distributions and reactivity coefficients are shown for different operating conditions on the examples of the representative UOX and MOX fuel assemblies. The effects of the multigroup energy structure of the cross section library, the self-shielding options and the choice of the calculation model are analysed. By the comparison to the Monte Carlo reference, the APOLLO2 code shows the high capability of prediction and analysis of the BWR reactor physics.

Key Words: APOLLO2, BWR

1. INTRODUCTION

The general purpose transport code APOLLO2 [1] is widely used for the analysis of light water reactors, both in research organisations and in industry [9]. The detailed multigroup cross sections libraries, the powerful self-shielding model, the robust flux solvers and leakage models, together with the implemented homogenization and flux reconstruction techniques, allow for a wide range of applications [2]. The calculations with different levels of physical modelling can be performed, from direct, detailed in space and detailed in energy calculations, which can reach the precisions close to those of Monte Carlo results, to the faster calculations that are based on a variety of homogenisation and/or flux reconstruction techniques which are performed in fewer energy groups [8]. The employ of the code for the analysis of the BWR assemblies under different operating conditions has been significantly ameliorated by the introduction of a new self-shielding model that takes into account the resonance interferences [6], and the new highly efficient acceleration techniques for the flux solver based on method of characteristic (MOC) [3, 4]. Also, the recent improvements over the standard 172 group XMAS multigroup structure by using the SHEM energy mesh, which extends the input library to 281 groups [7], makes possible to circumvent the self-shielding calculation for energies below 22.6 eV.

In this paper we show the capability of APOLLO2 to correctly predict the reactivity, pin power distributions and reactivity coefficients for a wide range of BWR operating conditions, from the cold state to hot, 100 % voided, with the control rod inserted, or the cold situation with the boron injected. We compare the results with the Monte Carlo reference code TRIPOLI4 [5], using different levels of modelling related to the self-shielding, spatial mesh for the MOC flux solver and those devoted to the CPU time saving approximations.

The representative results are given for two different types of UOX and one MOX assembly configuration.

The example calculations of a 8×8-1 BWR fuel assembly show that the maximum pin power error can be reduced to 1.5 %, and the reactivity coefficients show a good agreement with the Monte Carlo reference.

2. DESCRIPTION OF THE FUEL ASSEMBLIES AND CALCULATION OPTIONS

The two UOX assemblies, shown in Fig. 1, are identified as 8×8-1 and 8×8-2 types, both having 8 by 8 lattice positions. The 8×8-1 type is a simple configuration which contains one water rod and one gadolinium pin with 2.5 % of Gd_2O_3. The other lattice positions are occupied by the fuel of three different enrichments between 1.5 and 2 %. The 8×8-2 type assembly contains two water rods and the UOX pins with six different enrichments in ^{235}U varying form 1.6 % to 3.6 %. Six pins contain 3.5 % of Gd_2O_3. The MOX assembly has the geometry of an ATRIUM-10 type with the material properties taken from the specification of the NEA BWR MOX Benchmark Problem [11].

A typical run of APOLLO2 used for the assembly spectrum calculation consists mainly of two parts: the first is the self-shielding and the second is the flux calculation with a chosen leakage model. These are repeated for each burn-up step or for each state point in a series of branch calculations.

The direct calculation employs a detailed in space self-shielding model with several tens self-shielding regions. Typically, and in the cases presented here, there are four regions for each representative standard fuel pin and eleven in a pin containing the burnable absorber. The pins may be grouped according to initial fuel type or similar environment. The flux solver in this case, is usually based on the method of characteristics, using several thousands flux regions and the multigroup structure of the basic cross sections library, which can be either of 172 or 281 energy groups.

In the fast industrial schemes, the simplifications are made in the geometric representation used for the self-shielding calculation. Also, the direct flux solution is replaced by an approximate one, which is based on the flux reconstruction techniques and can involve different flux solvers each using a different spatial representations and a different number of groups [8].

2.1. Self-shielding

The self-shielding model accounts for spatial dependency by means of collision probabilities which can be calculated on the exact or approximate model problem geometry. Fast collision probability solutions can be obtained using the interface current approximation on a simplified geometry. The simplification is done by ”cell mixing” i.e. by imposing the same flux value in the cells that have similar isotopic composition and environment. This significantly reduces the number of flux regions but still handles properly the Dancoff effect. During the depletion calculation, all fuel pins undergo a different isotopic change, and for the needs of self-shielding, the pins with the average content must be calculated.

The code allows to user to set-up its own self-shielding model by choosing the geometry and the isotopes to be taken into account, together with the related energy interval and slowing down model. The options have been optimized in order to well represent the physics of all possible BWR operating conditions and to maintain a reasonable CPU time cost. The self-shielding in the examples shown is calculated for ^{235}U and ^{238}U, plutonium isotopes, from ^{238}Pu to ^{242}Pu, and gadolinia, from ^{155}Gd to ^{158}Gd. The mutual shielding for the overlapping resonances is taken into account selectively in two energy ranges for XMAS library as shown in Table I, and only in the first interval using SHEM, as there is no self-shielding calculation below

22.6 eV. The interface current approximation is used for the collision probability calculation, with the currents represented as uniform in space and P_1 in angle on cell interfaces.

2.2. Spatial mesh

The spatial mesh in routine calculations is usually parameterized using a predefined meshing pattern. For the fuel pins it is convenient to use the same division into concentric annuli following the definition of the self-shielding and depletion regions. The mesh applied in here described calculations uses four and eleven annuli, respectively for an ordinary fuel pin and a Gd-pin. Three annuli in water of each pin cell are used to represent the gradients next to the fuel and there is a single region in the clad. The gadolinium bearing rod is divided into eleven annuli. The whole cell is then divided in eight sectors that are positioned as shown in Fig. 2.

3. RESULTS

The results are compared with the TRIPOLI4 reference. In order to assure the consistency of the basic nuclear data used in the APOLLO2 and TRIPOLI4 codes, the same evaluation file, JEF2.2, has been chosen. Also, the same data processing system which is developed at CEA and based on NJOY has been used, with the only difference in treatment being in final placing into multigroup form for APOLLO2.

All TRIPOLI4 calculations used 600 batches of 5×10^4 particles each, with the first 200 batches discarded in order to get the pin-wise reaction rate distributions. The uncertainty on the multiplication factor in all cases does not exceed 25 pcm and it is approximately 0.2 % for the pin by pin fission rates.

3.1. Influence of self-shielding geometry

The influence of the spatial refinement on the self-shielding is shown on the example of 8×8-2 UOX assembly, which is tested for three different geometry representations. The choice of ”cell mixing” for the three investigated cases was as follows: In the case 1, besides the water holes, each self-shielding cell type coincides with a fuel cell type (enrichment), which represents 6 different fuel cells in geometry for self-shielding calculation. The second case comprises 9 different fuel cell types, where the cells next to the Gd-bearing pins are split in different cell types. Finally, the third case with 11 fuel cell types was obtained by distinguishing two more cells neighbouring the water rods.

The calculation was carried out using 172 group library and the flux solution was seek on a spatial mesh with 8 sectors times 4 annuli in ordinary fuel cell and with 11 annuli in Gd-pin cells. Tables II and III show respectively, the reactivity and fission rate errors in comparison with TRIPOLI4 reference. It can be noticed that the maximum reactivity error does not exceed 180 pcm. The pin wise fission rates are practically insensitive to the geometry model used, and the fission rate errors extrema are identical at 0.1 % precision, so the Table III is representative for all three cases. On the contrary, one observes a significant sensitivity of the pin capture rates to the geometry model for higher void fractions. This is shown in Table IV and it can be explained by a bigger importance of the epithermal neutron spectrum when the void fraction increases and the self-shielding effects need a more accurate treatment.

3.2. Spatial mesh and multigroup structure

The calculations on the example of an 8×8-1 case showed here, were performed using directly the method of characteristics in both 172 (XMAS library) and in 281 energy groups (SHEM), and with two different spatial meshes. The configuration without and three configurations with control rods are considered with three different control blades containing the B_4C absorber. All of them have the same design as shown in Fig. 2, and only the diameter of the absorber pin differs.

The spatial mesh for the MOC solver is presented here in two variants. The first comprises 2522 regions, where the mesh for fuel cells is the one described in previous section and shown in Fig. 2. The width of water gaps is subdivided in three layers. The second mesh contains 3419 regions and is obtained by refinement of the first one. All periphery fuel pins receive twelve sectors and the width of the water gaps is subdivided in six layers. This mesh tends to represent better the thermalization peaks in the water gaps, especially for cold states.

The results are given for ten different states which are identified by the Legend on the page 6. Two cold states identified as "cold" and "isothermal" correspond to the temperature of 293 K and 373 K respectively. Two different hot temperatures, designated as "nominal" and "Doppler", are used with different void fractions, and a configuration with the injected boron corresponds to "cold" temperature. The reactivity errors and pin-wise fission rate errors are shown respectively on Figs. 3 and 4. The values correspond to ten different states in four configurations ("uncontrolled" and with three kinds of control rods: rod "v1" to "v3"). The four diagrams on each figure show the four different calculations, two-by-two using the SHEM and XMAS libraries and two different spatial meshes. The Fig. 4 shows that the SHEM energy structure improves the precision of the pin rate distributions for the hot states and high void fractions, while the maximum error of -2 %, which happens to be in the corner pin, still remains for the spatial mesh of 2522 regions regardless of library. This error is reduced to 1.5 % using the refined spatial mesh for the MOC solver. This mesh refinement describes better the thermal flux gradients, which are significant in the vicinity of peripheral cells, and which augment in the absence of void, especially in cold condition when the water density is increased.

3.3. Reactivity coefficients

The void reactivity coefficient is defined here as $\Delta k_{\text{eff}}/\Delta v$, where v is the void fraction. The absolute discrepancies are expected to be less than 1 % or 1000 pcm. The errors in void fraction are presented in Tables V and VI for respectively 8×8-1 and ATRIUM-10-MOX assemblies in terms of absolute difference in pcm from TRIPOLI4 values. It can be noted that the SHEM mesh gives a better prediction for highly voided situation (80 % to 100 %).

The percent errors of control rod worth for cold state and hot operating conditions are shown in Table VII for the 8×8-1 assembly. The case corresponds to XMAS library and 3419 regions spatial mesh. It can be seen that the errors do not exceed 1.5 %. The errors for the ATRIUM-10-MOX are shown in Table VIII.

The reactivity errors of the ATRIUM-10-MOX calculations are shown in Table IX. These calculations were run with the XMAS library and the "standard" spatial mesh, i.e. with eight sectors in the periphery cells. It can be noted that in the worst case, which is the cold state with the control rod inserted, the error is not bigger than 300 pcm.

4. CONCLUSIONS

The APOLLO2 code is shown to produce highly accurate results when applied to BWR assemblies. The results presented, based on the use of the recent developments, show a very good agreement with the Monte Carlo reference. In all cases shown it is possible to reduce the error at less than 300 pcm in reactivity and less than 2 % in pin-wise fission rates. An increased number of groups is needed in some situations to improve the results, like the 281 group SHEM energy mesh in hot states, while the numerical approximations such as spatial mesh, are relevant in other conditions.

The future optimisations will use the latest developments of the MOC solver for APOLLO2, which is based on a linear flux approximation [10], and will allow to reduce significantly the number of flux regions while preserving the target precision.

All presented calculations used the cross section libraries issued from JEF2.2 evaluation. The newly generated libraries are based on JEFF3.1 and the validation process is in progress.

REFERENCES

[1] R. Sanchez et al., "APOLLO II: A user-oriented, portable, modular code for multigroup transport assembly calculations," *Nucl. Sci. Eng.*,**100**, pp. 352 (1988).

[2] S. Loubiere, et al., "Apollo2 Twelve Years Later", *M&C'99 Topical Meeting* , Madrid, Spain, September 27-30 (1999).

[3] R. Sanchez and A. Chetaine, "A synthetic acceleration for a two-dimensional characteristic method in unstructured meshes," *Nucl. Sci. Eng.* ,**136**, 122 (2000).

[4] S. Santandrea, R. Sanchez, "Analysis and improvements of the DPn acceleration technique for the method of characteristics in unstructured meshes", *Ann. of Nucl. Energy*, **32**, p. 163-193 (2005).

[5] J.P. Both et al., "A survey of TRIPOLI-4," *Proceedings of the 8th International Conference on Radiation Shielding*, Arlington, Texas, April 24 (1994).

[6] M. Coste-Delclaux, S. Mengelle, "New Resonant Mixture Self-Shielding Treatment in the Code APOLLO2", *PHYSOR-2004*, Chicago IL, April 25-29, (2004).

[7] N. Hfaiedh and A. Santamarina, "Determination of the Optimized SHEM Mesh for Neutron Transport Calculation", *Proc. of Int. Conf. on Math. and Comp., React. Phys. and Nucl. Appl. M& C2005*, Avignon (France), September 12-15, (2005)

[8] I. Zmijarevic, E. Masiello, R. Sanchez, "Flux reconstruction methods for assembly calculations in the code APOLLO2", *PHYSOR-2006*, Vancouver, BC, Canada, September 10-14, (2006).

[9] V. Marotte et al, "Industrial application of APOLLO2 to Boiling Water Reactors", *PHYSOR-2006*, Vancouver, BC, Canada, September 10-14, (2006).

[10] S. Santandrea and P. Mosca, "Linear Surface Characteristic Scheme for the Neutron Transport Equation in Unstructured Geometries", *PHYSOR-2006*, Vancouver, BC, Canada, September 10-14, (2006).

[11] "Physics of Plutonium Recycling − Volume VII: BWR MOX Benchmark − Specification and Results", *OCDE/NEA*, (2003).

Table I. Energy range for mutual shielding calculations using two libraries.

interfering isotopes	energy range bounds (eV) XMAS		SHEM	
	upper	lower	upper	lower
^{238}U+ ^{235}U+ ^{239}Pu+ ^{240}Pu	204.	33.72	241.2	33.72
^{238}U+ ^{235}U+ ^{240}Pu	22.63	19.45		

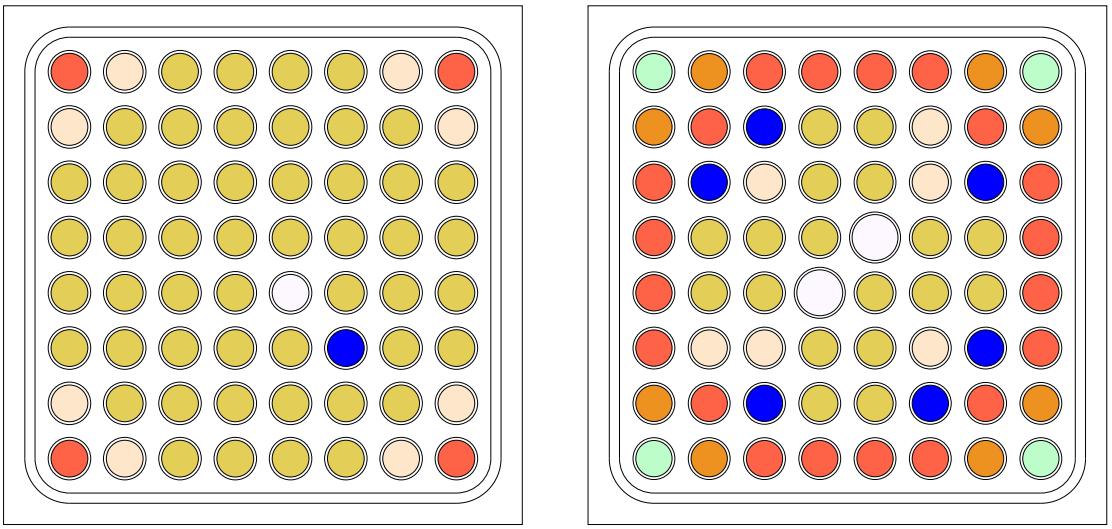

Figure 1. Two UOX assemblies: 8×8-1 (left) and 8×8-2 (right). The colours represent different fuel types. Gadolinium pins are in blue, water rods in white.

Color legend for plots:
– cold, – isothermal,
– 0% nominal, – 40% nominal, – 80% nominal, – 100% nominal,
– 0% doppler, – 40% doppler, – 80% doppler,
– boron.

Table II. 8×8-2 assembly: reactivity errors (in pcm) for three different geometry refinements in self-shielding.

number of cells	state				
in self-shielding	cold	0%	40%	80%	100%
6	−112	−133	−130	−156	−165
9	−113	−134	−134	−162	−176
11	−113	−135	−134	−162	−174

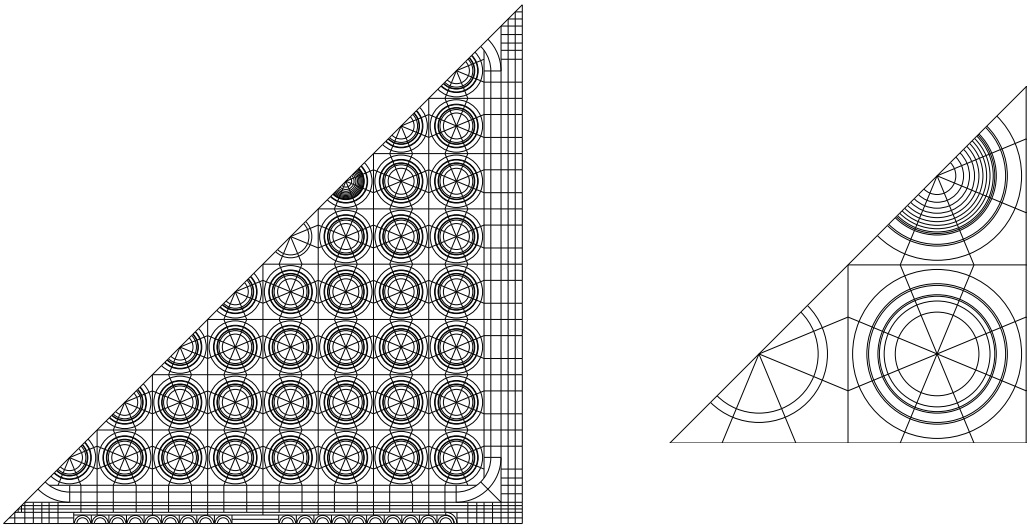

Figure 2. Spatial mesh for the MOC calculation (left) and an enlarged detail in the vincinity of the Gd pin (right).

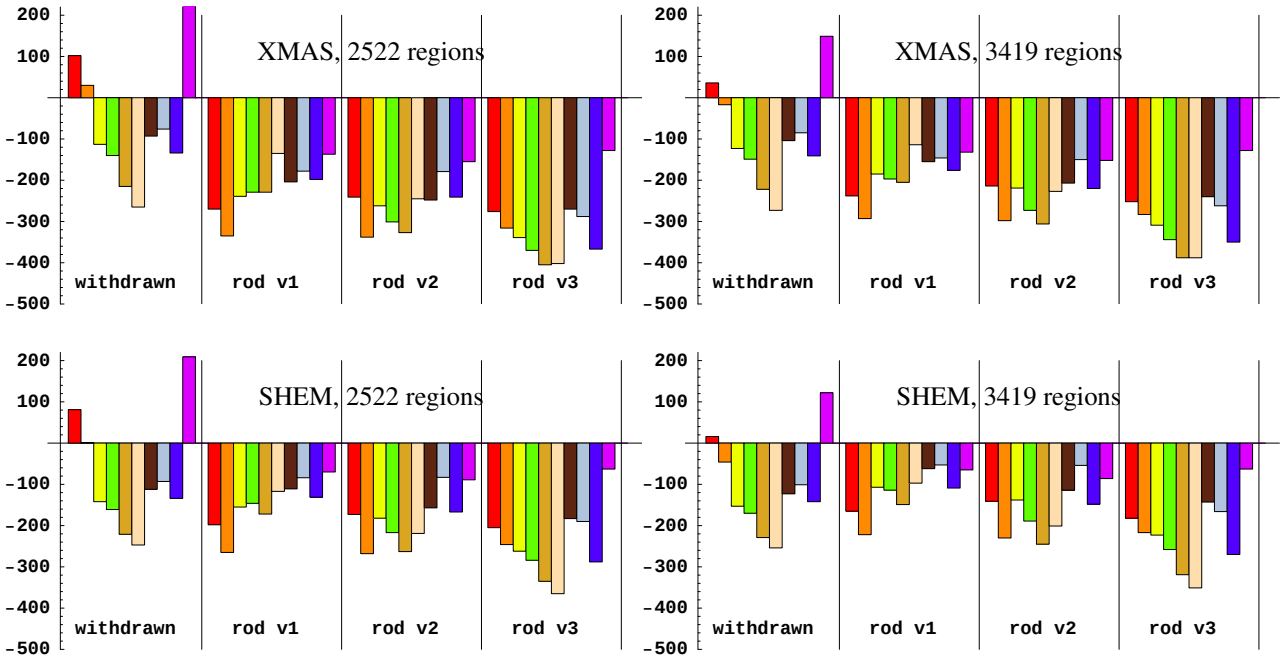

Figure 3. 8×8-1 assembly: reactivity errors (in pcm) for four assembly configurations in ten different states. Calculations done with XMAS and SHEM libraries for two different spatial meshes. Each state is assigned a color defined in Legend on page 6.

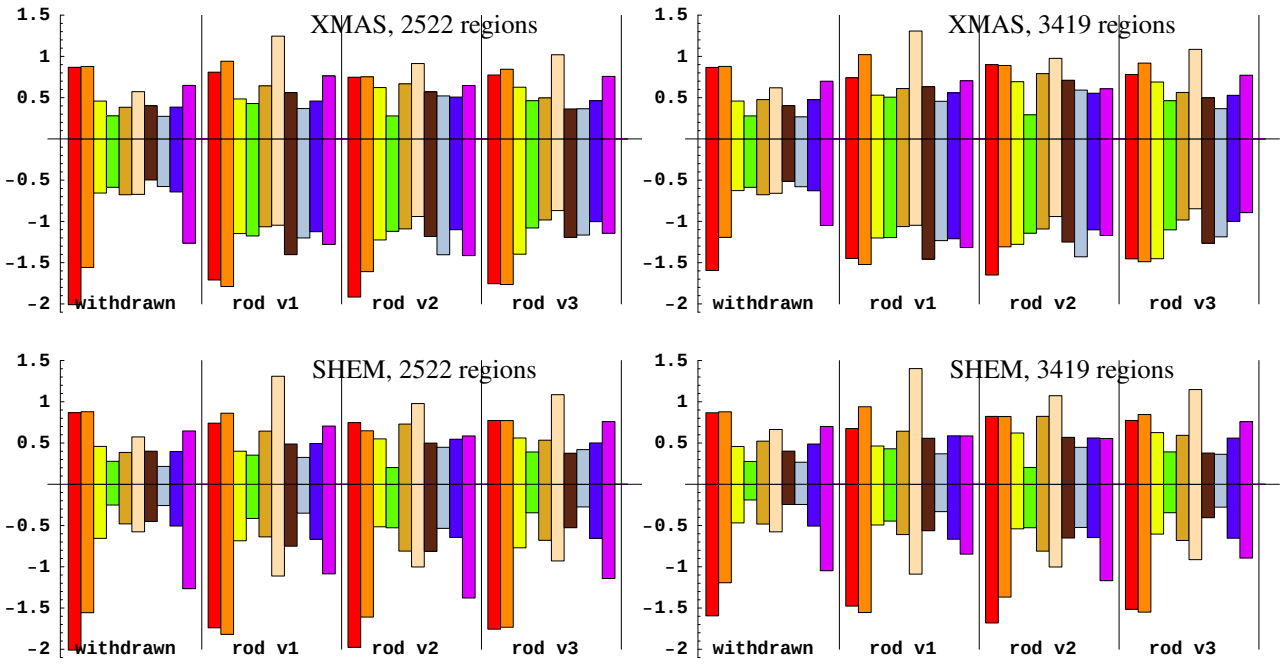

Figure 4. 8×8-1 assembly: error bounds (in %) of pinwise fission rate for four assembly configurations in ten different states. Calculations done with XMAS and SHEM libraries for two different spatial meshes. Each state is assigned a color defined in Legend on page 6.

Table III. 8×8-2 assembly: error bounds (in %) of pin-wise fission rates.

	state				
	cold	0%	40%	80%	100%
max. upper	2.1	1.2	0.6	0.5	1.0
max. lower	−2.4	−1.2	−0.5	−0.7	−0.8
RMS (%)	1.0	0.5	0.2	0.4	0.5

Table IV. 8×8-2 type assembly: error bounds (in %) of pin-wise capture rate for three different geometry refinements in self-shielding.

6 cells	state				
in self-shielding	cold	0%	40%	80%	100%
max. upper	2.3	1.8	2.3	2.9	3.9
max. lower	−1.6	−0.9	−0.5	−1.0	−1.5
RMS (%)	0.9	0.7	0.7	1.0	1.4
9 cells	state				
in self-shielding	cold	0%	40%	80%	100%
max. upper	2.3	1.9	1.6	2.0	2.4
max. lower	−1.6	−0.9	−0.5	−0.7	−1.2
RMS (%)	0.9	0.6	0.6	0.6	0.8
11 cells	state				
in self-shielding	cold	0%	40%	80%	100%
max. upper	2.3	1.9	1.7	1.4	1.7
max. lower	−1.6	−0.9	−0.5	−0.5	−0.4
RMS (%)	0.9	0.6	0.5	0.5	0.6

Table V. Void coefficients for 8×8-1 assembly: absolute errors in pcm.

rod	void change		
	0%-40%	40%-80%	80%-100%
	XMAS		
out	−68	−185	−225
v1	7	33	350
v2	−75	5	350
v3	−28	−2	115
	SHEM		
out	−38	−142	−90
v1	3	−32	210
v2	−80	−55	215
v3	−40	−52	−15

Table VI. Void coefficients for ATRIUM-10-MOX assembly: absolute errors in pcm. The calculations used XMAS energy mesh.

rod	void change	
	0%-40%	40%-80%
out	−20	−10
cr1	−42	179

Table VII. Control rod worth for 8×8-1 assembly: relative percent errors.

rod type	state				
	cold	0%	40%	80%	100%
v1	1.2	0	0	−0.1	−0.2
v2	1.1	0.1	0.1	0.1	0
v3	1.4	0.4	0.3	0.2	0.2

Table VIII. Control rod worth for ATRIUM-10-MOX assembly: relative percent errors. The calculations used XMAS energy mesh.

rod type	state			
	cold	0%	40%	80%
cr1	−0.5	−0.8	−0.7	−0.8

Table IX. Reactivity errors (in pcm) for ATRIUM-10-MOX assembly.

rod type	state			
	cold	0%	40%	80%
out	156	−115	−121	−121
cr1	269	88	74	167